Mon. Not. R. Astron. Soc. **000**, 1–18 (2007) Printed 19 September 2007 (MN LATEX style file v2.2)

Observational evidence for AGN feedback in early-type galaxies

Kevin Schawinski[1⋆], Daniel Thomas[2,1], Marc Sarzi[3,1], Claudia Maraston[2,1], Sugata Kaviraj[1], Seok-Joo Joo[4], Sukyoung K. Yi[4] and Joseph Silk[1]

[1]*Department of Physics, University of Oxford, Oxford OX1 3RH, UK*
[2]*Institute of Cosmology & Gravitation, University of Portsmouth, Portsmouth, PO1 2EG, UK*
[3]*Centre for Astrophysics Research, Science & Technology Research Institute, University of Hertfordshire, Hatfield, UK*
[4]*Center for Space Astrophysics, Yonsei University, Seoul 120-749, Korea*

Submitted 2007 August 1, Accepted 2007 September 11.

ABSTRACT

A major amendment in recent models of hierarchical galaxy formation is the inclusion of so-called AGN feedback. The energy input from an active central massive black hole is invoked to suppress star formation in early-type galaxies at later epochs. A major problem is that this process is poorly understood, and compelling observational evidence for its mere existence is still missing. In search for signatures of AGN feedback, we have compiled a sample of 16,000 early-type galaxies in the redshift range $0.05 < z < 0.1$ from the SDSS database (MOSES, Morphologically Selected Ellipticals in SDSS). Key in our approach is the use of a purely morphological selection criterion through visual inspection which produces a sample that is not biased against recent star formation and nuclear activity. Based on the nebular emission line characteristics we separate between star formation activity, black hole activity, the composite of the two, and quiescence. We find that emission is mostly LINER-like in high-mass galaxies ($\sigma > 200$ km/s) and roughly evenly distributed between star formation and AGN at intermediate and low ($\sigma < 100$ km/s) masses. The objects with emission (~ 20 per cent) are offset from the red sequence and form a well-defined pattern in the colour-mass diagram. Star forming early-types inhabit the blue cloud, while early-types with AGN are located considerably closer to and almost on the red sequence. Star formation-AGN composites are found right between these two extremes. We further derive galaxy star formation histories using a novel method that combines multiwavelength photometry from near-UV to near-IR and stellar absorption indices. We find that in those objects deviating from the red sequence star formation occurred several 100 Myr in the past involving $1-10$ per cent of the total stellar mass. We identify an evolutionary sequence from star formation via nuclear activity to quiescence. This transition process lasts about 1 Gyr, and the peak AGN phase occurs roughly half a Gyr after the starburst. The most likely interpretation is that star formation is suppressed by nuclear activity in these objects before they settle on the red sequence. This is empirical evidence for the occurrence of AGN feedback in early-type galaxies at recent epochs.

Key words: galaxies: active, galaxies: elliptical and lenticular, galaxies: evolution, galaxies: formation, galaxies: active

1 INTRODUCTION

The formation of early-type galaxies is one of the major unsolved problems of astrophysics. Despite their apparent simplicity, they have time and again refused to fit into the bigger picture and thus, they have been the most difficult and illuminating test for galaxy and structure formation theory. In every generation of theoretical models, early-type galaxies have helped provide the insights into what physics was still missing from them and they continue to do so. The vast majority of early-type galaxies appear to have formed most of their stars at high redshift on very short timescales as suggested by the stellar population properties of nearby samples (e.g. Trager et al. 2000; Thomas et al. 2005; Nelan et al. 2005; Bernardi et al. 2006; Jimenez et al. 2006) as well as the redshift evolution of luminosity and mass functions of massive galaxies (e.g. Wake et al. 2006; Cimatti et al. 2006; Rodighiero et al. 2007a).

Until very recently, the predictions from semi-analytic models of hierarchical galaxy formation were in severe conflict with the observationally derived formation ages and timescales of early-type

⋆ E-mail: kevins@astro.ox.ac.uk (KS)

galaxies. These models take the merger trees of dark matter haloes in a ΛCDM universe either by following them in a cosmological N-body simulation (Kauffmann et al. 1999)) or generating them using the extended Press-Schechter formalism (White & Frenk 1991). They then calculate the more complex fate of baryonic matter inside them with prescriptions for star formation (Kennicutt 1998), radiative cooling of gas (Sutherland & Dopita 1993; Springel et al. 2001) and feedback from supernovae (Kauffmann et al. 1999). Early semi-analytic models such as that of Kauffmann & Charlot (1998) predicted that the most massive galaxies in the universe harbour the youngest stellar populations and assemble the last, contrary to what has been deduced from observations. For a critical example, these models struggle to match the observed chemical abundance ratios and their trends with galaxy mass (Thomas 1999; Nagashima et al. 2005).

The reason for this failure in the early models is that star formation continues unchecked in massive haloes where supernova feedback is insufficient (Dekel & Silk 1986). Benson et al. (2003) showed that in massive galaxies, an additional, more powerful heating source than SNe is needed to heat the cold gas that fuels star formation and therefore stop it. This additional heating source is now generally identified as feedback from active galactic nuclei (AGN) where jets and outflows from the central supermassive black hole are presumed to heat and expel most residual gas via a wind thus preventing further star formation. This *AGN feedback* has been discussed by a number of authors (Ciotti & Ostriker 1997; Silk & Rees 1998; Binney 2004; Springel et al. 2005a; Silk 2005) and is now part of many galaxy formation models (Granato et al. 2001, 2004; Springel et al. 2005b; Kaviraj et al. 2005; Croton et al. 2006; Bower et al. 2006; De Lucia et al. 2006; Cattaneo et al. 2006, 2007; Cavaliere & Menci 2007; Kawata & Gibson 2005). The phenomenological model of Schawinski et al. (2006b) is specifically motivated by *GALEX* observations of early-type galaxies. Di Matteo et al. (2005) and Springel et al. (2005a) have also investigated the effect of AGN feedback in hydro simulations of mergers and have now placed them in large-scale simulations probing cosmological volumes (Di Matteo et al. 2007; Sijacki et al. 2007). Note that alternatives have been suggested based on the processes of cooling and shock-heating of baryonic matter in dark matter haloes (Birnboim et al. 2007; Khochfar & Ostriker 2007; Hopkins et al. 2007).

AGN feedback may come in two different modes at different epochs during cosmic time. In an early phase at high redshifts the AGN may truncate and quench star formation leading to the formation of the dominant old population in massive galaxies. This so-called 'quasar mode' (Croton et al. 2006) is most likely accompanied by vigourous black hole growth and leads to very strong *kinetic* feedback that quenches strong starbursts. The other face ofAGN feedback can be thought of as a 'maintenance' mode. It turns on at more recent epochs such that furthersignificant episodes of star formation are prevented (Best et al. 2005, 2006; Fabian et al. 2005, 2006). The coupling between the black hole accretion and the gas heating is poorly constrained by the observation. The latter mechanism has only recently been included in semi-analytic galaxy formation models. While such prescriptions are successful at curing some key issues, their major problem is that the physics of this process is still poorly understood and essentially unconstrained by observations. Compelling observational evidence for the *mere existence* of AGN feedback in early-type galaxies is still missing.

The aim of this paper is to tackle the key question of the role of AGN feedback observationally by looking for its signatures in early-type galaxies at recent epochs in the nearby universe. Crucial for this purpose is the compilation of a sample of early-type galaxies with a selection method that does not bias against AGN and/or star formation. The sample further needs to be large, because the potentially short duration of the AGN feedback phase makes such objects relatively rare. To this end we have constructed a sample of nearly 16,000 early-type galaxies from the Sloan Digital Sky Survey (SDSS) in the redshift range $0.05 \leqslant z \leqslant 0.1$. These early-types are part of a sample comprising 50,000 early- and late-type galaxies in that redshift range compiled in a project called Morphologically Selected Ellipticals in SDSS (MOSES, Schawinski et al., in preparation). The major novelty is the purely morphological selection mechanism through visual inspection of *all* 50,000 galaxies. Through emission line diagnostics we identify active early-type galaxies with star formation activity and/or AGN. From the stellar populations we derive star formation histories for these objects, which allows us to explore the possible interaction between the formation histories of the galaxies and their current star formation/AGN activities.

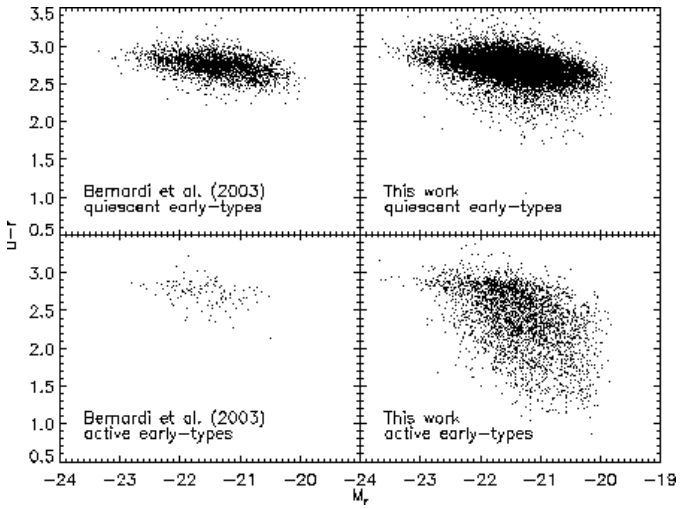

Figure 1. Optical colour-magnitude relation for the early-type catalogue of Bernardi et al. (2003a) and this work. Early-type galaxies are divided into 'quiescent' and 'active' depending on whether emission lines are detected. Our purely morphologically selected sample contains a significantly larger fraction of active early-type galaxies.

The paper is organised as follows. In Sections 2 and 3, we outline the sample selection, present the emission line diagnostics, and the stellar population analysis. We place the sample galaxies subdivided in quiescent, AGN, and star forming objects on the colour-σ relation and discuss first tentative conclusions in Section 4. A more quantitative discussion is provided in Section 5 based on the two-component star formation histories derived. Conclusions in the context of AGN feedback in galaxy formation are discussed in Sections 6 and 7.

Throughout this paper, we assume a standard ΛCDM cosmology consistent with the WMAP results (Bennett et al. 2003) with $\Omega_m = 0.3$, $\Omega_\Lambda = 0.7$ and $\mathrm{H}_0 = 70\ \mathrm{h}_{70}\ \mathrm{km}^{-1}\ \mathrm{s}^{-1}$. All magnitudes are in the AB system.

2 DATA SAMPLE

The sample utilised here is part of a project called MOSES: **MO**rphologically **S**elected **E**llipticals in **S**DSS. Key is that all

48,023 galaxies in this sample have been visually inspected and classified into early- and late-type morphology by eye, yielding a sample of 15,729 early-type galaxies. A detailed description of the catalogue can be found in a companion paper (Schawinski et al., in preparation), and we refer the reader to this paper for any details. In the following, we provide a brief summary with focus on the aspects that are most relevant for the present work.

2.1 Sample Selection

We use the Sloan Digital Sky Survey DR4 as our main sample (York et al. 2000; Stoughton et al. 2002; Adelman-McCarthy et al. 2006). The *SDSS* is a survey of the Northern Sky providing us with photometry in the five filters *u,g,r,i* and *z* (Fukugita et al. 1996; Gunn et al. 1998). We selected objects from the redshift slice $0.05 < z < 0.10$ with the magnitude limit $r < 16.8$. These cuts are mostly motivated by the limit out to which a visual inspection of galaxy morphology is reliable (see Schawinski et al. 2006a).

2.2 Morphological Classification

The selection criteria used to identify early-type galaxies are crucial. Selection criteria based on galaxy properties such as colour, spectral features or concentration index rather than morphology are at risk to be biased against early-type galaxies with residual star formation or AGN activity. As these are the objects most relevant for the present study, we decided for a radical, purely morphological selection.

The first catalogues of early-type galaxies in the *SDSS* used for extensive study are those of Eisenstein et al. (2001) and Bernardi et al. (2003a,b,c,d). The Bernardi et al. (2003a) catalogue is based primarily in the likelihood of the surface-brightness profile resembling a de Vaucouleurs law and a high concentration index. This is a very efficient way of selecting large numbers of spheroids, but can fail to reject spiral galaxies with prominent bulges. In particular, spirals with face-on faint disks and edge-on disks can pass these criteria. Furthermore, Bernardi et al. (2003a) reject galaxies with a PCA classification number atypical of red, passive early-types (Connolly & Szalay 1999). This means that early-types with strong emission lines or that are dominated by young stellar populations are rejected despite having early-type morphology. For an example, the early-type galaxies discussed by Fukugita et al. (2004) would not be included. Recently, Fukugita et al. (2007) have compiled an catalogue of morphological early-type galaxies by visual inspection of 2,658 objects from the *SDSS*.

For the MOSES sample we carried out manual inspection of multi-colour images from SDSS by eye *for all 48,023 galaxies*, in order to avoid any potential bias introduced by selecting by colours or spectral features. We define as early-type galaxies all objects earlier than and including S0 galaxies and reject galaxies from our sample if they show distinct spiral arms or a disk. We *include* in this selection objects with clear tidal features or other signs of morphological disturbance. In the paper presenting the MOSES catalogue (Schawinski et al., in preparation) we present a number of example images from *SDSS* to illustrate the effectiveness of our visual inspection. Out of the 48,023 galaxies in our volume limited sample, we identify 15,729 early-type galaxies. Figure 1 illustrateSs the difference between our selection and that of Bernardi et al. (2003a) in the colour-σ diagram. It can be seen clearly that our morphological selection yields a significantly higher fraction of early-type galaxies with emission lines and/or blue colours. Less than 5% of the early-type galaxies in the catalogue of Bernardi et al. (2003a) show emission lines, while over 18% of ours do.

2.3 Photometry

We retrieved *SDSS* model magnitudes (`modelMag`) for all five filters *u,g,r,i* and *z* from the *SDSS* DR4 database. In order to improve the wavelength coverage of the galaxies in our sample, we match them to a number of other surveys, namely *GALEX*, *2MASS*, and *SWIRE*.

2.3.1 Matching to GALEX

The **Galaxy Evolution Explorer** (*GALEX*; Martin et al. 2005) is conducting several surveys of the ultraviolet sky in two filters: far-UV (*FUV*; 1344-1786Å) and near-UV (*NUV*; 1771-2831Å). The *Medium Imaging Survey* from the General Release 3 (MIS/GR3) is covering a portion of the sky coinciding with the *SDSS* to a limit of 23 AB in *NUV* and *FUV*. We match our galaxies to MIS within $4''$ to find counterparts. GR3 only covers a fraction of *SDSS* DR4 and so this matching gives us detections for 13.4% of galaxies.

2.3.2 Matching to 2MASS

The **Two Micron All Sky Survey** (2MASS; Skrutskie et al. (2006)) provides us with *J*, *H* and K_s band imaging for our galaxies selected in *SDSS*. We match our galaxies to the *Extended Source Catalogue* (XSC) within $4''$, giving us counterparts for 87.1%. The *2MASS* photometry is done in the Vega system, so in order to keep consistency with the rest of the MOSES sample, we convert the magnitudes from Vega to AB following Blanton et al. (2003a, 2005).

2.3.3 Matching to Spitzer-SWIRE

The **Spitzer Wide Area Extra-galactic Survey** (SWIRE; Lonsdale et al. 2003) is one of the Spitzer Legacy Surveys and imaged nearly 50 square degrees using both the IRAC ($3.6, 4.5, 5.8, 8.0\mu$m) and MIPS ($24, 70, 160\mu$m) instruments. We cross-match the MOSES sample to the public source catalogues for ELAIS N1, N2 and Lockman Hole fields. Only a small fraction of our sample (0.3%) has counterparts at 3.6μm.

2.4 Spectroscopy

SDSS has performed follow-up spectroscopy using $3''$ fibres yielding a reasonably complete sample to $r < 17.77$ (Blanton et al. 2003b). The spectra cover the range of 3800 to 9200Å at a resolving power of 1800 and for the MOSES sample have a typical signal-to-noise of about 30. We retrieve the *SDSS* optical spectra for all our galaxies.

2.4.1 Gas and stellar kinematics

We measure the kinematics of the stars and the emission-line fluxes of our galaxies from their SDSS spectra following the methods

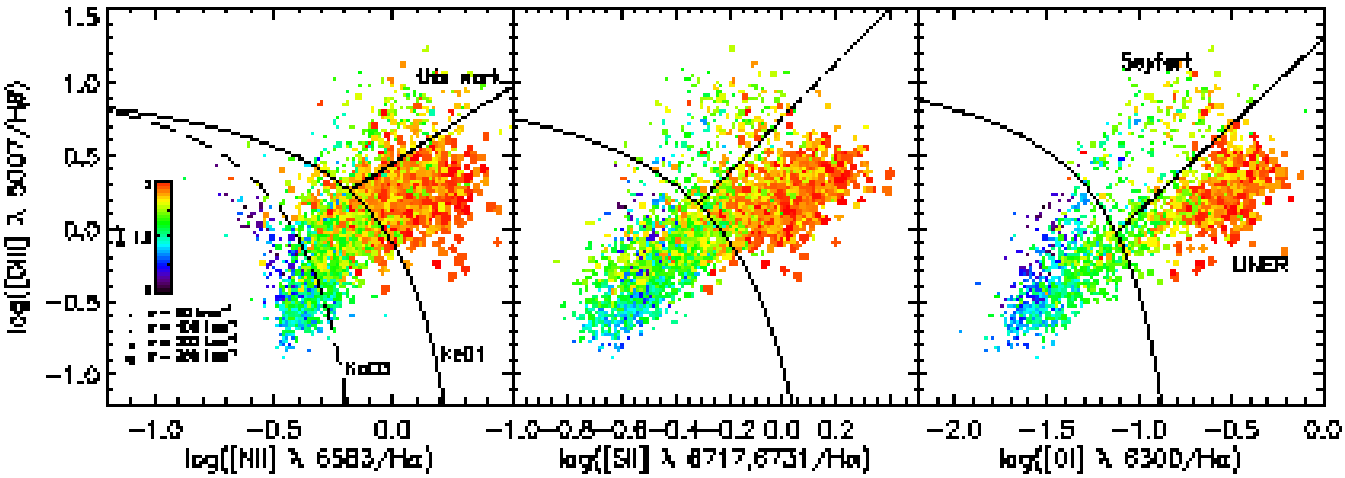

Figure 2. The BPT line diagnostic diagrams for the early-type galaxies of the MOSES sample. Each galaxy is coloured by its optical u-r colour (see colour bar in left-hand panel). Point sizes scale with the galaxy velocity dispersion as an indicator of mass (see legend in left-hand panel). In each diagram, we indicate the demarcation lines used in our classification scheme. The dashed line in the [NII]/Hα diagram (left-hand panel) is the empirical star formation line of Kauffmann et al. (2003) (labelled Ka03), while the solid curve (in all three panels) is the theoretical maximum starburst model from Kewley et al. (2001) (labelled Ke01). The galaxies in between these two lines are SF-AGN composites or 'transition region objects'. Galaxies below the Ka03 line are dominated by star formation. The division line between Seyferts and LINERs is shown as the straight line following Kewley et al. (2006) for the middle and right-hand panel and our own definition (see text) for the left-hand panel.

of Cappellari & Emsellem (2004) and Sarzi et al. (2006), respectively[1]. We separate the contribution of the stellar continuum and of the ionised-gas emission to the observed galaxy spectrum by fitting *simultaneously* stellar population templates (from Tremonti et al. 2004) and Gaussian emission-line templates to the data. In these fits we account also for the impact of diffuse dust in the galaxy of dust in the emission-line regions, which allows to obtain a decrement on the strength of the Balmer lines that is at least what expected by recombination theory. From the fit to the stellar continuum and absorption features, we measure the line-of-sight velocity dispersions. From subtraction of the emission-line spectrum from the observed one, we get the clean absorption line spectrum free from emission line contamination. We then use this cleaned spectrum to measure the stellar absorption indices. The physical constraints on the emission from high-order Balmer lines ensures the strength of the corresponding absorption features is correctly estimated, which is crucial for constraining the ages of stellar populations.

2.4.2 Lick absorption line indices

On each spectrum we measure the 25 standard Lick absorption line indices (Worthey et al. 1994; Worthey & Ottaviani 1997) following the most recent index definitions of Trager et al. (1998). For this purpose the spectral resolution is reduced to the wavelength-dependent Lick resolution (Worthey & Ottaviani 1997). The measurements are then corrected for velocity dispersion broadening. The correction factor is evaluated using the best fitting stellar template and velocity dispersion obtained previously. Errors are determined by Monte Carlo simulations on each spectrum individually based on the signal-to-noise ratios provided by the *SDSS*. Possible discrepancies between the flux-calibrated *SDSS* spectral system and the Lick system are negligible, as shown in a detailed analysis of Lick standard stars observed with *SDSS* (Carson 2007).

2.5 Emission line diagnostics

Emission line diagnostic diagrams are a powerful way to probe the nature of the dominant ionising source in galaxies (Baldwin, Phillips, & Terlevich 1981, hereafter BPT). They allow the separation of galaxies into those dominated by ongoing star formation and non-stellar processes; and with sufficient information can further split those into Seyfert AGN and LINERs[2]. The diagrams also contain a transition region, where the emission lines indicate a blend of star formation and AGN activity.

We use the four optical line ratios [OIII] λ5007/Hβ, [NII] λ6583/Hα, [SII] λ6583/Hα and [OI] λ6583/Hα. We follow the signal-to-noise criterion of Kauffmann et al. (2003) and classify all galaxies that have a S/N $>$ 3 detection of Hα, Hβ, [OIII] λ5007 and [NII] λ6583. The two low ionisation species [SII] and [OI] are used when detected, as they are usually weaker than the other four.

2.5.1 Diagnostic diagrams

The corresponding three diagnostic diagrams are shown in Fig. 2. Each galaxy is coloured by its optical $u-r$ colour. Point sizes scale with the galaxy velocity dispersion as an indicator of mass. In each diagram, we indicate the demarcation lines used in our classification scheme. In the left-hand column, we show the [NII]/Hα diagram used to separate star forming objects (blue) by means of the demarkation line by Kauffmann et al. (2003, dashed line). We verified that the somewhat more restrictive separation between star forming and AGN suggested by Stasińska et al. (2006) does not alter the results of this work. The remaining objects are divided in composite Transition Region objects (purple) and AGN using

[1] We made use of the corresponding `ppxf` and `Gandalf` IDL codes adapted for dealing with SDSS data. Both softwares can be retrieved at http://www.strw.leidenuniv.nl/sauron/

[2] LINER: low ionisation nuclear emission line region

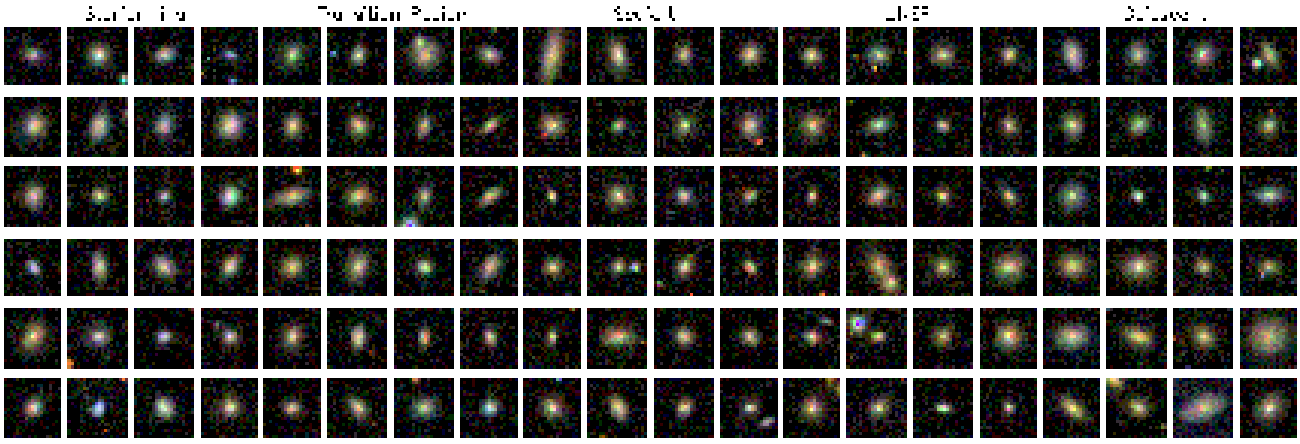

Figure 3. A sample of morphological early-typegalaxies from the MOSES sample sorted by their emission line classification. The cutouts are $40h^{-1}$ kpc by $40h^{-1}$ kpc in size.

the theoretical maximum starburst model from Kewley et al. (2001, solid lines).

The AGN are then further sub-classified into Seyferts (green) and LINERs (red) by the straight solid lines. The more indicative low ionisation species (middle and right-hand panel) are used where possible. The best separation of Seyferts and LINERs is achieved using [OI] (right-hand panel of Fig. 2), which is used wherever [OI] is detected with S/N > 3. The [OI] line is generally weaker then any of the other emission lines used, so where it is not available, we use [SII]. To separate the two types of AGN, we use the lines defined by Kewley et al. (2006). If both these lines are not detected we adopt the original [NII] diagram for AGN classification. Based on the location of those galaxies classified by [OI] or [SII] on the [NII] diagram, we define a new empirical Seyfert-LINER separation:

$$\log([\mathrm{OIII}]/\mathrm{H}\beta) = 1.05\,\log([\mathrm{NII}]/\mathrm{H}\alpha) + 0.45 \quad (1)$$

2.5.2 *Classification results*

Following the emission line classification we divide our early-type galaxy sample into five classes.

(i) Quiescent (orange)
(ii) Starforming (blue)
(iii) Transition Region (purple)
(iv) Seyfert (green)
(v) LINER (red)

Most objects in the quiescent early-type galaxy class are virtually free of emission lines. A small sub-fraction exhibits weak [OIII] emission, but lack the other emission lines necessary for the BPT classification. We verified that a further separation of this subclass does not affect the results of this work. The quiescent objects make up the bulk of the early-type population (82 per cent). The early-type galaxies with significant emission lines (S/N > 3 in the four main BPT lines) represent the remaining fifth of the early-type sample. We call these active early-type galaxies, and separate them into star forming, transition objects, Seyferts and LINERs. The results of this classification are summarised in Table 1. For further details we refer the reader to the paper describing the MOSES catalogue (Schawinski et al, in preparation). We show some example images of morphological early-type galaxies in Figure 3.

Table 1. Emission Line Classification Results

Classification	Number	Fraction Galaxies	Colour
Early-type galaxies	15729	100%	
Quiescent	12828	81.5%	orange
Starforming	671	4.3%	blue
Transition Region	1087	6.9%	purple
Seyfert	242	1.5%	green
LINER	901	5.7%	red

2.5.3 *Star formation rates*

For those galaxies classified as starforming, we derive star formation rates from the extinction-corrected Hα line luminosity according to the conversion of Kennicutt (1998). All star formation rates for our galaxies quoted in this paper are based on Hα unless otherwise noted. We cannot derive reliable star formation rates for any of the other emission line classes, as an unknown fraction of the Hα emission line is of non-stellar origin.

3 STELLAR POPULATION ANALYSIS

The spectrum of a galaxy contains a record of its star formation history over the age of the universe. Its stellar populations are the combination of all the episodes of star formation that a galaxy and its progenitors underwent. Reconstructing this star formation history or at least recovering it partially is a challenging task that requires excellent observational data, stellar population models for the interpretation and a statistically sound method for the recovery.

For the problem at hand in this paper, we turn to the parametric approach. It has been used with great success by Ferreras & Silk (2000) and by Kaviraj et al. (2006) to use the immense discriminating power of restframe near- and far-UV photometry to test whether individual early-type galaxies have undergone episodes of recent residual star formation or not.

3.1 Two-Component star formation histories

The aim of this work is the mapping of current star formation/AGN activities in galaxies with their star formation histories. Of particu-

lar relevance for us is the epoch and the strength (hence mass fraction) of the last significant starburst that occurred in a galaxy. Since the most recent episode of star formation dominates the spectrum at all wavelengths, it is the easiest to recover (see Figure 4). Following the approach of Kaviraj et al. (2006), we therefore fit two-component star formation histories to the galaxy data.

The old component is modelled as an instantaneous starburst of variable age and metallicity, and represents the formation of the bulk stellar population of the galaxy before the most recent episode of star formation. We allow this old component to vary between a t_o of 1 and 15 Gyrs. By marginalising over this parameter later on, we are summing all possible linear combinations of single starbursts and so take into account all possible star formation histories before the most recent starburst.

On top of this, we add a young component of a certain age t_y and mass fraction f_y. It turns out that this young burst is poorly modelled by an instantaneous starburst, so that we choose to represent it by an exponentially declining star formation rate with an e-folding time of 100 Myr. The choice of 100 Myr is motivated by a test on a small sub-sample, where we left the e-folding time τ as an additional free parameter. In this test, we recovered a typical τ of $\sim$100 Myr for early-type galaxies with young components, so we set τ to 100 Myr *a posteriori*. The parameter t_y stands for the look-back time to the beginning of the starburst, f_y is the total mass fraction formed in the recent burst extrapolating the 100 Myr e-folding star formation history to infinity. Since virtually all ages we recover for the starburst population are at least $\sim$100 Myr, the difference between the mass actually formed by today and the total mass that will form is small.

This parametric quantification of the age and mass fraction of the secondary population allows us to derive a *recent* star formation history against the background of any possible star formation histories in the distant past, represented by a simple stellar population (SSP), whose effect we can account for by marginalisation. This approach is different from purely non-parametric approaches in the literature that make no *a priori* assumptions on the star formation history to be recovered (e.g. Panter et al. 2003, 2006).

3.2 Internal metallicity distribution

Besides assigning an average metallicity to each model, we additionally consider the internal distribution of metallicities necessarily present in each galaxy. This is important, as a tail of low metallicity stars can have a significant effect in particular on the ultraviolet part of the spectrum (Maraston & Thomas 2000). We construct an analytic form of the typical metallicity distribution from observations of the bulge of M31 and the closest early-type galaxy NGC 5128 where individual stars can be resolved (Sarajedini & Jablonka 2005; Harris et al. 1999; Harris & Harris 2000, 2002). This metallicity distribution is modelled with two Gaussians. The bulk metallicity is a Gaussian with a mean metallicity μ_Z and a spread of σ = 0.22 dex, while the tail is parametrised as a Gaussian shifted by 0.75 dex to lower metallicity with the much larger spread of σ = 1.5 dex. Both components are such metallicity composites, and we vary μ_Z to cover a mean mass-weighted metallicity $Z(\mu_Z)$ ranging between $\sim 1/200 Z_\odot$ to $\sim 3.5 Z_\odot$.

3.3 Dust extinction

Internal dust extinction causes a degeneracy with age and mass that needs to be taken into account. To describe dust attenuation we adopt the extinction law by Calzetti et al. (2000). This choice is mainly motivated by the fact that the active early-type galaxies in our sample are undergoing significant episodes of star formation, so that an extinction law derived from a sample of starforming galaxies seems reasonable. In separate runs we have tested a number of other extinction laws (Milky Way (Allen 1976), LMC (Fitzpatrick 1986), SMC (Prevot et al. 1984; Bouchet et al. 1985) and verified that in general, the Calzetti et al. (2000) law provides the best fits. The dust parameter E(B-V) is varied between 0.0 and 0.8.

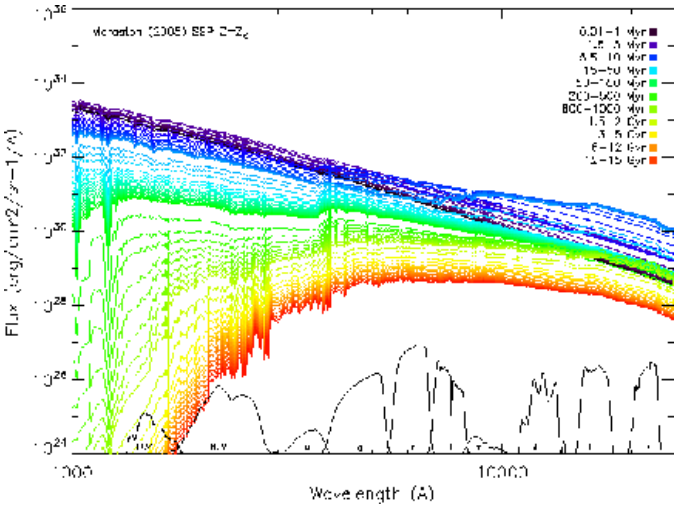

Figure 4. The pace of stellar evolution: we show the SED of a solar metallicity M05 SSP from 0.01 Myr to 15 Gyr. The different ages are colour-coded and we indicate the filters we use by their filter transmission curves of the data we use in this paper at the bottom. The broadband colours of a galaxy will always be dominated by the youngest stellar population formed in the most recent episode of star formation. Any older population will be small by comparison even with respect to a relatively small young mass-fraction. This feature of stellar evolution allows us to effectively split the star formation history into two components until about 1.5-2 Gyr when the pace of stellar evolution slows down and populations of different ages up to 15 Gyr become similar and the differences are on the order of the effects of dust and metallicity.

3.4 Combining photometry and spectroscopy

A crucial novelty of our approach is the combination of photometric and spectroscopic data, which increases the power of breaking the degeneracies between age, mass, metallicity and dust content. The reason why this helps is that the degeneracies are different because of the dissimilar *non-linear* responses of broadband colours and stellar absorption indices to these parameters. Like cosmologists who combine the very degenerate contours of one experiment with another to find a well-constrained set of parameters in the intersection, we harness two very different observables that couple to the fundamental physical parameters in very different fashions.

It should be noted that, absorption line indices are not significantly affected by dust (MacArthur 2005). A further cornerstone in our fitting algorithm for the identification of intermediate-age populations is the inclusion of near-IR photometry and stellar population models (Maraston 2005) that adequately describe the thermally pulsing asymptotic giant branch (TP-AGB) phase. This is crucial as the TP-AGB provides most of the near-IR light of a stellar population between 0.5 to 2 Gyr (Maraston 1998).

In a nutshell, we perform a comparison of the observed photo-

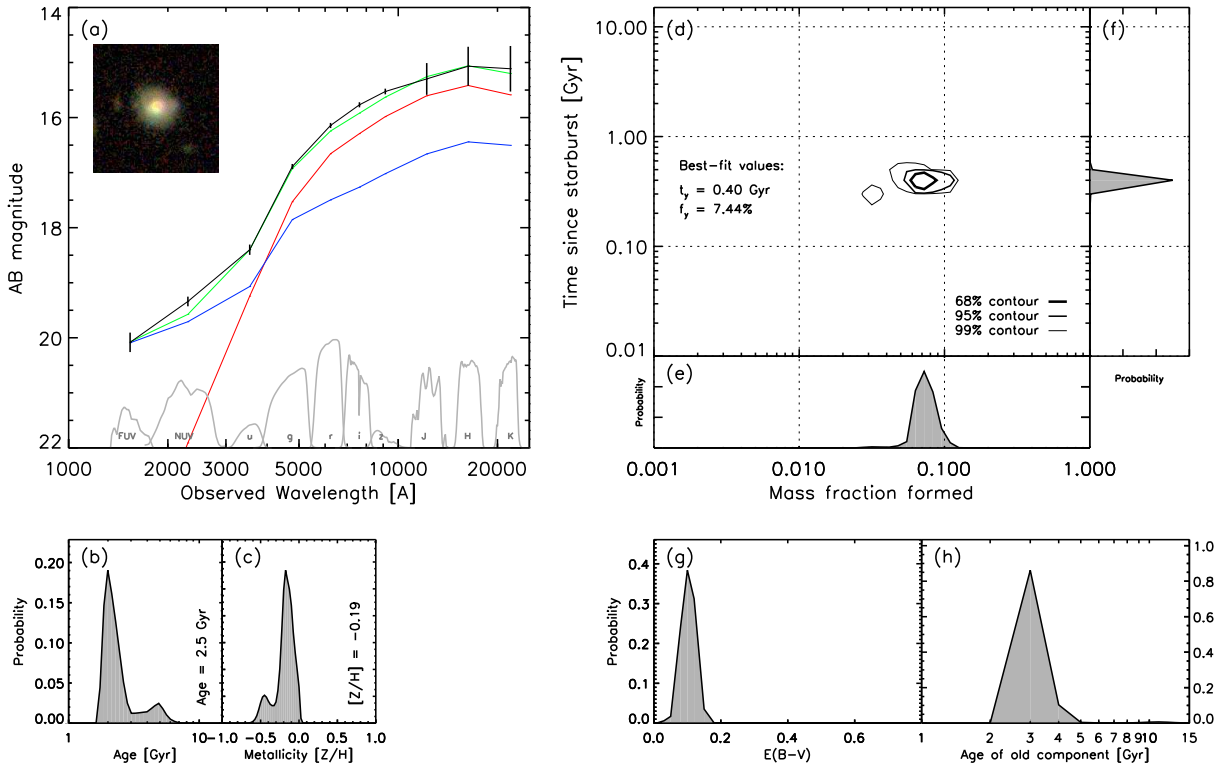

Figure 5. An example of a galaxy where we can resolve and quantify the last significant episode of star formation. This object is a Starforming early-type galaxy. For a detailed description, see section 3.5.

metric SED (of as many as are available of *FUV, NUV, u, g, r, i, z, J, H, K*) to a library of SEDs of over five million two-component star formation histories from Maraston (2005) and compute the appropriate model SED parameterised by the five parameters described above (t_y, f_y, t_o, μ_z and $E(B-V)$) compute the associated χ^2 statistic to obtain a probability distribution function for those five parameters. An intrinsic error for our photometry across all filters of 0.015 mag is adopted to deal with the uncertainties in the absolute photometric calibration of *SDSS*

Simultaneously, we compute the associated luminosity-weighted SSP ages and metallicities for each model. We derive luminosity-weighted SSP ages and metallicities by χ^2 fitting the Thomas et al. (2003, 2004) models to the 25 Lick absorption line indices and compute a second probability distribution through the comparison of these quantities with the V-luminosity weighted ages and metallicities of the photometric comparison. These two probability distributions from the SED and absorption line fitting are then convolved to the final one.

In order to estimate the parameters of interest, we marginalise the resulting 5-dimensional probability distribution function to obtain the two-dimensional distribution in the recent starburst age vs. mass-fraction plane (t_y-f_y). We integrate over this surface to obtain confidence levels constraining the age and mass-fraction of the last significant episode of star formation in the galaxy. These probability distributions are stacked to get typical values for the subpopulations.

3.5 Example galaxies

In this section we present two example fits to galaxies with very different properties and star formation histories. The first galaxy is an active early-type in the transition region of the emission line classification which suggest that the object is dominated both by ongoing star formation and an AGN. Its Hα star formation rate is 2.1 $M_{\odot}yr^{-1}$ and its UV-optical colours place it squarely into the blue cloud ($u-r$ = 2.3, $NUV-r$ = 3.2). The second galaxy is a typical passive quiescent early-type galaxy with no detected emission lines. Its UV-optical colours place it on the red sequence ($u-r$ = 2.8, $NUV-r$ = 6.1). The availability of *GALEX NUV* and *FUV* photometry generally improves the confidence contours, but does not shift the best fit.

The fit results are summarised in Figs. 5 and 6. In panel (a) we show the fit to the photometry: in black are the observed broadband colours with the errors magnified by a factor of 3 to make them visible. To guide the eye, we show the filter transmission curves of the various filters used from *GALEX* far-UV to *2MASS* K-band. The best-fit model is shown in green and the separate old and young components are red and blue respectively. We also show the *SDSS* colour images.

In panels (b) and (c) we show the probability distributions for the luminosity-weighted age and metallicity derived from the absorption line indices. The final result in the t_y-f_y plane is shown in panel (d). This plot quantifies strength and epoch of most recent episode of star formation. In panels (e) and (f), we show the projected, projected probability distributions for the parameters t_y and f_y. In the main analysis we will stack these distributions for various

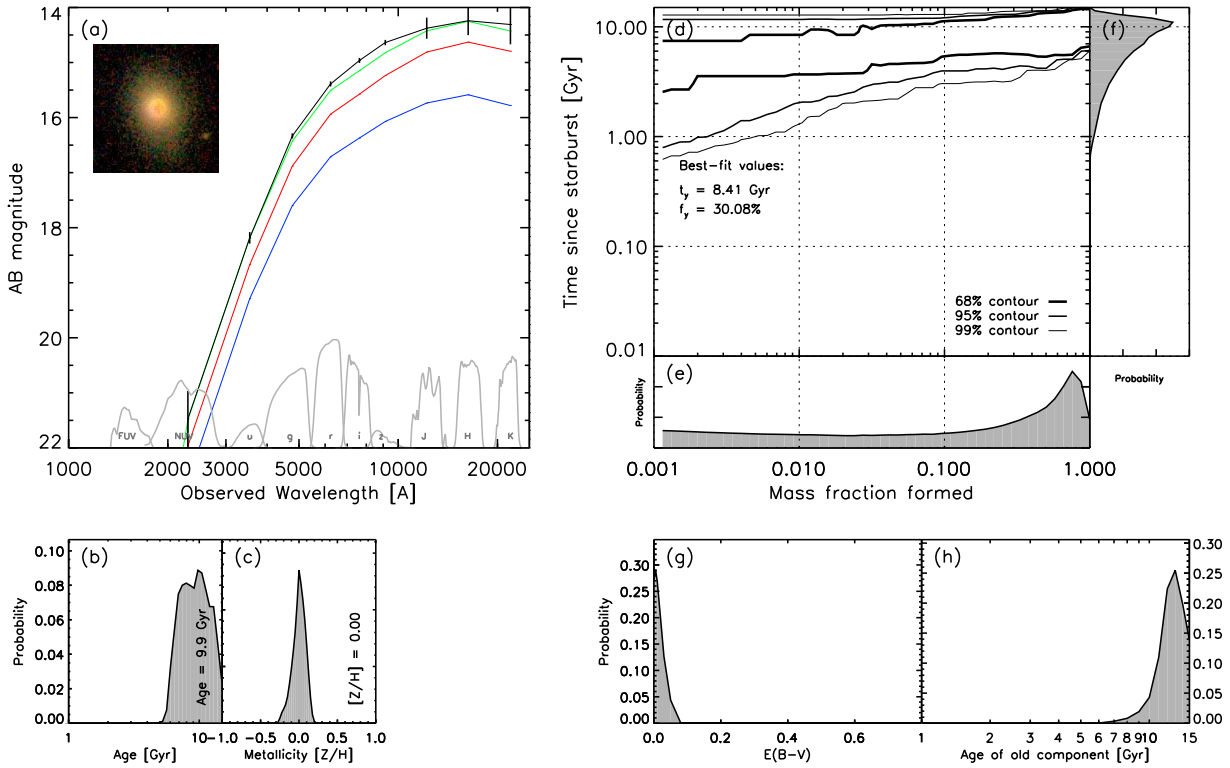

Figure 6. An example of a galaxy where we cannot quantify the first significant episode of star formation, but can place strong limits on the recent star formation history. For a detailed description, see section 3.5.

classes of galaxies. In panels (g) and (h), we show dust extinction $E(B-V)$ and the age of the old component.

The two example galaxies show very different star formation histories. The active galaxy has a very young luminosity-weighted age, which is well consistent with the increased UV flux. The two-component SED fit yields an old component of 3 Gyr and places the most recent starburst at an age of 400 Myr with a mass fraction of 7 per cent. Its dust content is relatively high ($E(B-V) = 0.1$) in agreement with the current star formation activity. The low luminosity-weighted age of the 'old' component implies that this object had several rejuvenation events in the past.

The emission line free galaxy, instead, has an old luminosity-weighted age derived from the spectroscopic data. The two-component fit yields basically two old components with ages around 10 Gyr. We can conclude that this galaxy clearly has not undergone a significant starburst in the recent past, while the details of its star formation history in the more distant past are not resolved. The 99% confidence intervals exclude any sort of significat star formation activity in the recent past. The very low dust attenuation value fits well into this picture.

We also note that while only a fraction of the galaxies in our sample have *GALEX*, their fitted star formation histories do not differ significantly from those without.

4 RED SEQUENCE AND BLUE CLOUD

In this Section, we discuss the position of the various galaxy classes defined through the emission line diagnostics in the colour-mass relation. This simple comparison allows us to draw first tentative conclusions that are independent of our stellar population analysis method. Quantitative results of the detailed analysis will be presented in the subsequent section.

4.1 Active galaxies in the colour-mass relationship

In Fig. 7 we show *u-r* colour as a function of galaxy velocity dispersion σ for the galaxies in our sample. The morphological late-type galaxies are shown as grey points, the early-type galaxies are coloured points subdivided in the various emission line classes: quiescent (i.e. no emission lines, orange), LINER (red), Seyfert (green), Transition (purple), and star forming (blue). The quiescent early-type galaxies (see most right-hand panel) form the well-known red sequence, while the late-type galaxies in the sample define the so-called blue cloud (grey points).

The first key result of this work is that the active galaxies are offset from the red sequence and exhibit well-defined patterns across the colour-σ diagram. Starforming objects inhabit the blue cloud. While this may seem like an obvious result, note that the broadband SED and the emission lines probe very diffierent physical components of a galaxy. While the former traces the stellar populations and therefore the past, fossil record, the emission lines provide information on the *current* state of the *ionised gas* in the galaxy. It is very reassuring that objects with ongoing star formation show significant rejuvenation also in their stellar populations.

More importantly, those objects not dominated by star formation but by AGN activity, Seyferts and LINERs, are located considerably closer to and almost on the red sequence. Transition objects, instead, which are composites of star formation and AGN activity are found right between these two extremes. There is a

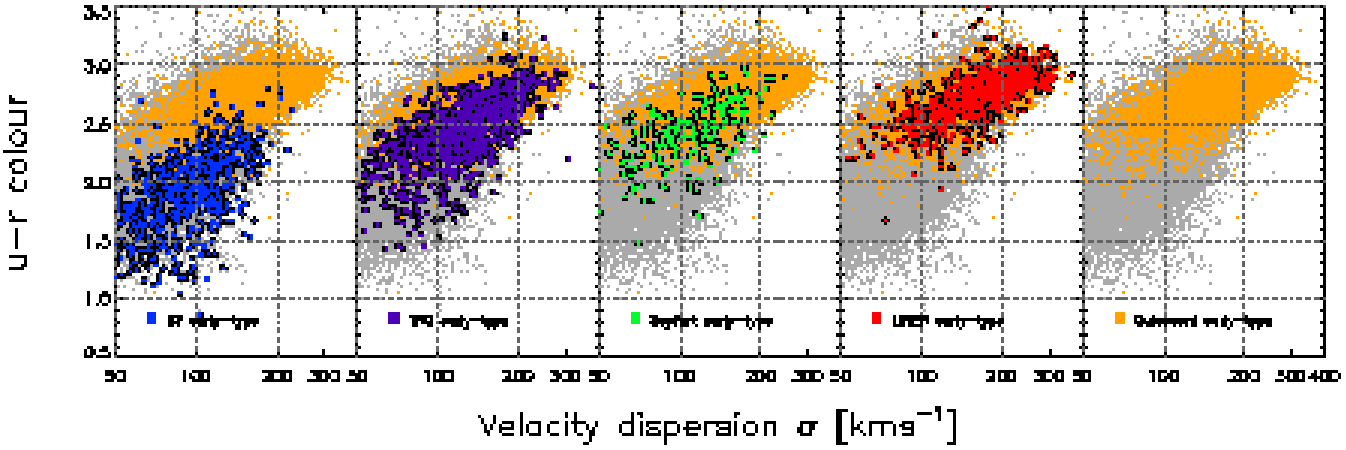

Figure 7. The colour-sigma relation for our sample. In each panel, morphological late-types are grey, quiescent early-types are orange and the various active early-types are blue (Starforming), purple (transition region), green (Seyfert) and red (LINER). The mass tracer is the stellar velocity dispersion.

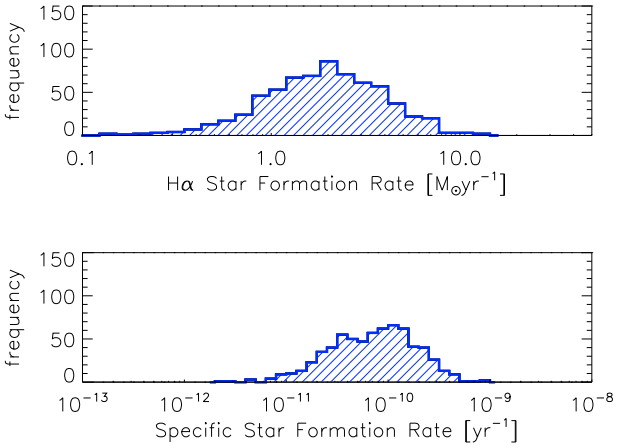

Figure 8. Histogram of the star formation rate and specific star formation rate of the Starforming early-type galaxies. The star formation rate is based on the luminosity of the Hα line and is converted to a rate using the relation of Kennicutt (1998).

sequence between the blue cloud and the red sequence from star forming via transition region and AGN to quiescence. In more general terms, the presence of AGN in a *green valley* between the blue cloud and the red sequence has been discussed in other recent work in the literature (Faber et al. 2005; Kauffmann et al. 2006; Martin et al. 2007; Nandra et al. 2007; Salim et al. 2007; Wild et al. 2007; Graves et al. 2007).

4.2 Mass dependence

This tentative sequence is convolved with a clear mass dependence of the emission line classification. The blue star forming objects are found at the low-mass end, while the majority of early-type galaxies classified as LINERs lie at the high-mass end on the red sequence. Transition objects and Seyferts reside between these two extremes also in their galaxy mass distributions.

The presence of a significant fraction of low-mass early-type galaxies showing signs of ongoing star formation of a few $M_\odot$ per year (see Fig. 8) is a striking result, which is mostly the merit of the pure morphological selection strategy. Still, this result is not surprising. The *GALEX* UV satellite has found evidence for minor recent star formation in early-type galaxies (Yi et al. 2005), and the *SAURON* survey of 48 nearby elliptical and lenticular galaxies has shown that many of them have (often extended) emission lines and signs of recent star formation as well as CO emissions from molecular gas and atomic hydrogen indicating sometimes substantial reservoirs of gas (Sarzi et al. 2006; Morganti et al. 2006; Combes et al. 2007).

In general, low-mass early-type galaxies are well-known to show young stellar ages, emission lines and even ongoing star formation. This downsizing of galaxy formation, wherein the most massive galaxies harbour the oldest stellar populations is now generally accepted. Today's early-type galaxies in particular show a clear correlation between mass and age (Caldwell et al. 2003; Thomas et al. 2005; Nelan et al. 2005; Bernardi et al. 2006; Jimenez et al. 2006).

Fig. 7 shows that our sample comprises a large, statistical subsample of active early-type galaxies in the intermediate-mass and low-mass regimes ($\sigma \lesssim 200$ kms^{-1}) allowing us to study the interplay between star formation, nuclear activity, and quiescence in early-type galaxies. We note that many of the high-mass transition region objects are most likely misclassified LINERs. They do not have any starforming or Seyfert counterparts at the same mass.

4.3 AGN feedback in action?

At low and intermediate masses we can identify a sequence at a given mass from star formation via transition region and AGN activity to quiescence, which is echoed in a sequence from blue to red stellar populations. Taking *u-r* colour as a proxy for the stellar age and hence using the stars as cosmic clock, this is highly suggestive of an evolutionary sequence. We are observing the act of galaxy transformation from the star forming blue cloud via the green valley to the passive red sequence *in action*.

We interpret the deviation from the red sequence as rejuvenation due to a recent episode of star formation. On their way back to the red sequence, galaxies appear to pass through a phase of significant nuclear activity, as transition region objects and Seyferts have colours between the blue star forming and the red sequence objects. This indicates that AGN may have a decisive role to play in this transformation process. Fig. 7 suggests that residual star for-

mation and nuclear activity are connected in early-type galaxies. It is possible that the AGN actually suppress the star formation activity, and we are witnessing AGN feedback in action. Our sample represents the ideal laboratory to probe these processes.

It should be noticed that the massive early-type galaxies in our sample do not appear to be part of such transformation process. At the high-mass end only quiescent and LINER objects are found.

What needs to be shown is twofold. First, solid evidence for the presence of an evolutionary sequence for the low/intermediate-mass objects is required. To this end, we have derived detailed star formation histories using the method presented in section 3 focusing on the epochs and mass fractions of the most recent starburst. This allows us to investigate whether the galaxies of the various sub-classes in our sample truly belong to the same object type at different evolutionary stages. Second, the interaction between star formation and nuclear activity along this sequence must be investigated, with the aim to understand whether and how the two processes are related. These are addressed in the following sections.

5 THE EVOLUTIONARY SEQUENCE

Following the discussion of the previous section we divide our sample in three velocity dispersion bins ($\sigma \leqslant 100$, $100 < \sigma \leqslant 200$ kms^{-1}, $\sigma > 200$ kms^{-1}) representing low-mass, intermediate-mass, and massive early-type galaxies. Within each σ bin we maintain the 5 sub-classes: star forming, transition object, Seyfert, LINER, and quiescent. Within each of the 15 resulting sub-classes we stack the probability distributions for the star formation histories obtained in the analysis of Section 3. We marginalise over all parameters except the mass-fraction f_y and age t_y of the starburst component. The resulting contours of the probability distributions in the t_y-f_y plane are shown in Fig. 9. The panels are analogues to panel (d) of Figs. 5 and 6. The five columns show the various emission line classes, the rows are the three σ bins. A bar in each panel indicates the relative fraction of objects in this particular sub-class.

5.1 Evidence for the time sequence

The results shown in Fig. 9 allow one immediate conclusion. The star formation histories derived for the low-mass and intermediate-mass objects in our sample galaxies reveal clear evidence for the occurrence of a starburst between 100 Myr and 1 Gyr in the past involving a typical mass fraction of 1 to 10 per cent. This reinforces the interpretation of deviations from the red sequence in the colour-σ diagram (see Fig. 7) to be caused by recent rejuvenation events. Key are the epochs and mass fractions of this rejuvenation for the various emission line classes. While the starburst ages clearly increase from star forming via AGN dominated to quiescent in a continuous sequence from ~ 100 Myr to beyond 1 Gyr, the mass fractions remain the same. This points to the various emission line classes having undergone the equivalent rejuvenation event in the past, and the only feature differentiating the various classes is the time elapsed since that star formation episode. Hence, the objects of the various emission classes in the panels along one row in Fig. 9 are identical in terms of mass, morphology and star formation history, except that the epoch of the last starburst varies. This means we have resolved an evolutionary sequence, and what we are seeing is the process of rejuvenation in early-type galaxies at different evolutionary stages. This time sequence includes a phase of AGN activity along the way.

The fraction of objects taking part in this transformation is strongly dependent on mass. In the lowest mass bin about one third of the objects shows emission lines and is caught in the process of this transformation. This fraction drops to 13 per cent in the intermediate mass bin containing galaxies with $100 \leqslant \sigma < 200$ kms^{-1}. In the highest bin for objects with velocity dispersion above 200 $\mathrm{kms}^{-1}$the evolutionary sequence is not detected. At the high-mass end, the vast majority of galaxies is quiescent, and no recent starburst within the past few Gyrs has occurred. The small fraction of active galaxies is by far dominated by LINER-like emission, with some transition region objects that are in fact closer to the properties of LINERs (see section 6.5.3).

5.2 Timescales along the sequence

For the low- and intermediate-mass objects ($\sigma < 200$ kms^{-1}) we can now determine the relative and absolute timing of this transformation process. We marginalise over the mass-fraction and compute the stacked probability distributions of starburst ages for the various emission line classes. The result is shown in Figure 10 for the low- and intermediate-mass early-type galaxies in the left-hand and right-hand panels, while in Table 2, we give the figures in Myrs. In both mass bins, we can see the shift in the age of the last episode of star formation in a sequence as could already be seen from Figure 9. The star forming objects are clearly the ones most recently rejuvenated with starburst ages around $150 - 300$ Myr, with the latter increasing along the sequence from transition region through Seyfert and LINER to quiescent.

A global interpretation yields the following picture: The most common starburst age t_y for the transition region objects is around 300 to 500 Myr. Seyfert activity appears further 100 to 300 Myr later with starburst ages peaking at about 600 Myr. This phase is followed by LINER and quiescent with separations of a few 100 Myr, respectively. The widths of the distributions increase along this sequence from about 200 Myr for the star forming objects to $400 - 600$ Myr in the transition region and Seyfert objects. The phases involving nuclear activity, transition and Seyfert, appear to be of comparable length in time and must be a factor two to three longer than the star forming one. Note that the widths of LINERs and quiescent objects are much less well determined as they extend into the regime of old ages beyond 1 Gyr, in which the age resolution is significantly reduced.

The transition region and the Seyfert phases seem to overlap considerably, which suggests that objects at this point along the time sequence may switch back and forth between Transition Region (a mixture of AGN and star formation) and Seyfert phase (pure AGN). If this is the case, the Seyfert phase represents episodes of enhanced accretion onto the black hole between phases with lower levels of nuclear activity together with low residual star formation. The star formation we see in the Transition Region objects may even be *induced* by the (potentially) recurrent Seyfert state as the jets and outflows pile up gas before finally pushing it out (Silk & Rees 1998; Silk 2005).

Toward the end of the sequence, the transition from the high-ionisation Seyfert phase to quiescence passes through a phase of nuclear activity characterised by low-ionisation (LINER). In total, the transformation process from blue cloud to red sequence passing through nuclear activity takes about 800 Myr to 1 Gyr.

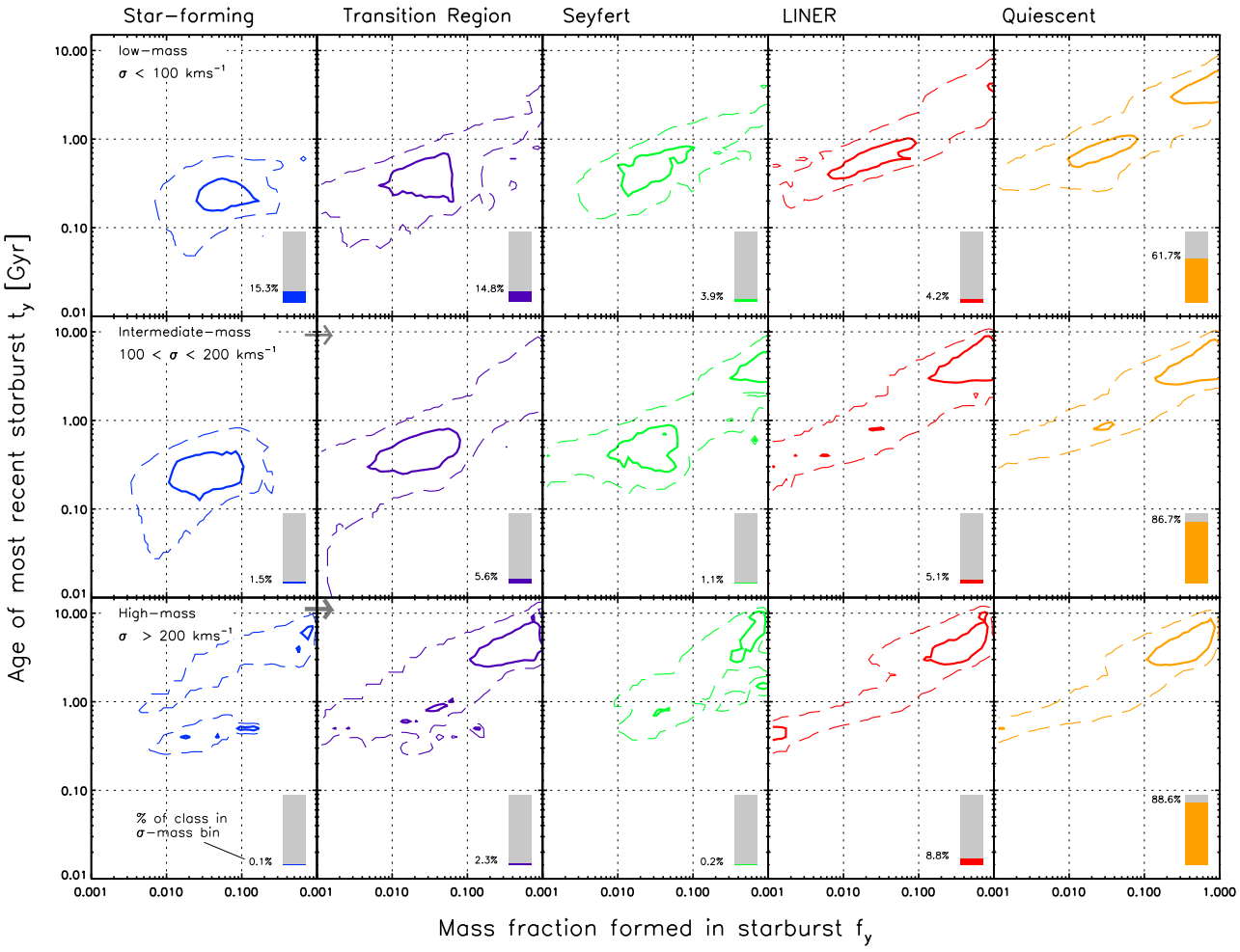

Figure 9. The recent star formation histories of early-type galaxies by mass and emission line class. In the horizontal direction, we split our sample into three velocity dispersion bins. Vertically, we split the galaxies in each σ bin by their activity type from Starforming to quiescent (c.f. Figure 7). The contours are 25% and 50% probability contours respectively. Note that the area of these contours can be misleading; only a small fraction of early-type galaxies is in classes other than the quiescent bin. In order to guide the eye, we indicate the fraction of galaxies in each mass bin (low, intermediate and high) that are in each emission line class. For example, in the high-mass regime, only a tiny fraction of early-types are classified as Starforming (most likely misclassifications), while the almost 90% are quiescent; nevertheless the contours occupy similar areas on the t_y- f_y plane.

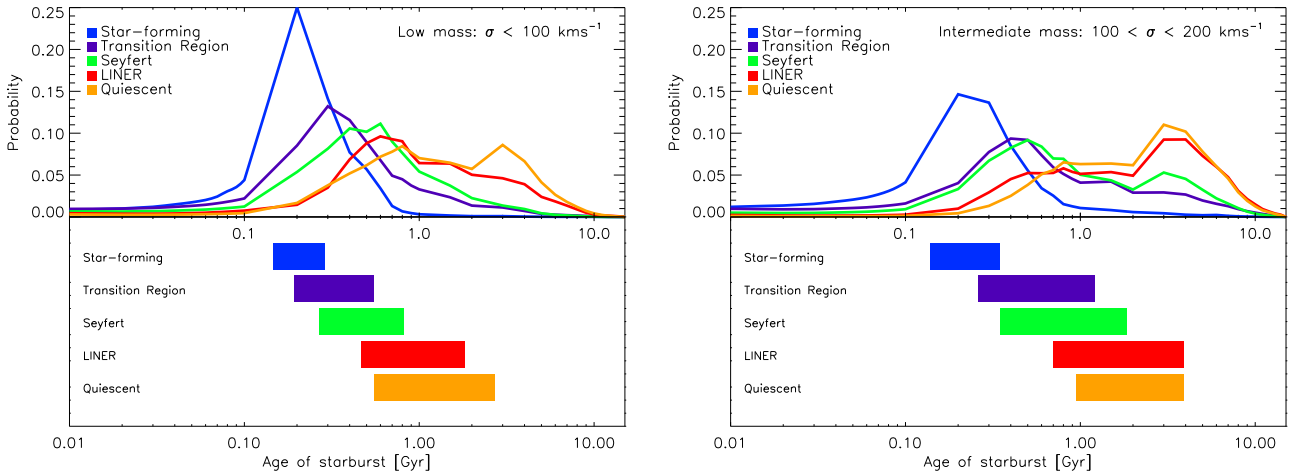

Figure 10. The time sequence in the low- and intermediate mass bin: In the top of each panel, we show the stacked, normalised probability distribution functions for the time elapsed since the start of the starburst t_y. In the bottom, we indicate where on the the t_y axis 50% of the probability lie. We give the numbers for this in Table 2.

Table 2. The Time Sequence: The Age of the Last Episode of Star Formation as a Function of Mass and Emission Line Class

Mass Regime	Velocity Dispersion kms^{-1}	Star Formation Myr	Transition Region Myr	Seyfert AGN Myr	LINERs Myr	Quiescent Myr
Low mass	0-100	145-280	195 - 550	270-800	470 - 1800	550-2700
Intermediate mass	100-200	140-350	260 - 1200	350-1800	700 - 4000	950-4000

The time intervals given in this Table correspond to the 50% probability intervals from Figure 10.

5.3 Lifetimes and number fractions

An important consistency check is the comparison of the lengths of the various phases as derived from the stellar population ages with the number of objects found in each phase. If the transition region and Seyfert phases are equally long, the number of objects found in these two classes must be the same. From Fig. 9 it can be seen that this is not the case. We observe three to four times more Transition Region objects than Seyferts. However, an unknown fraction of the objects in the Seyfert phase must be Seyfert Type I rather than Type II depending on the viewing angle from which the nucleus is seen. Indeed, broad emission line objects like Type I Seyferts are not classified as 'galaxies' by the *SDSS* spectroscopic pipeline and hence are not included in our sample. Thus, it is plausible that the ostensible lack of Seyfert AGN in our sample stems from this geometric effect, which puts object numbers and phase lifetimes in very good agreement. It should also be noted that our sample is not volume-limited.

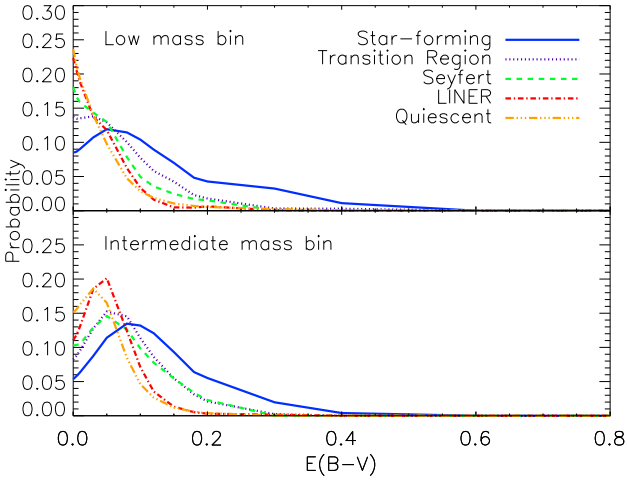

Figure 11. This plot shows the stacked, normalised probability distribution functions for the dust parameter $E(B-V)$ for the low and medium mass bin. Starforming early-types are the dustiest with the Transition Region and Seyfert early-types being less dusty and the LINERs and quiescent early-types containing even less dust.

5.4 Dependence on mass

The comparison between the lifetimes of the star forming and AGN phases is more complex, as an additional mass dependence comes into play. The fractions of the active early-type galaxy population in a given mass bin that are classified as transition region and Seyfert objects decrease by about a factor 2.5 from the low to the intermediate-mass bin, while the number of star forming objects decreases by a factor 7. This results in a factor 3.5 more transition region objects than star forming ones at intermediate masses, while their fractions are comparable at low masses. As the transition region phase lasts about two to three times longer than the star forming one in both mass regimes this suggests that not all low-mass objects go through the time sequence. Hence star formation is not followed by nuclear activity in all cases, and the true proportions between star forming and transition region objects for the SF-AGN sequence may be observed only at intermediate mass. This implies the presence of a tail of young quiescent objects in the low-mass bin, which is indeed indicated by the probability distributions in Fig. 10.

Still, the ratio transition region to star forming objects seems slightly too high at intermediate masses. The reason for this may be that some fraction of transition objects are misclassified and are actually LINERs (see 6.5.3) This would also explain why transition objects and Seyfert appear less well separated at intermediate mass.

Within these uncertainties, the fraction of galaxies that experiences residual star formation, and transitions from starburst to quiescence via nuclear activity drops by about a factor two to four between the low-mass and the intermediate-mass bins. The highest mass bin ($\sigma > 200$ kms^{-1}) concludes this trend, as no such sequence is detected for these masses. This is very well supported by the fact that the apparent dichotomy in the starburst age distribution within the quiescent early-types galaxies (left-hand panel of Fig. 10) is considerably weaker at intermediate masses (right-hand panel), and disappears entirely at the high-mass end (see Fig. 9).

Finally, it is interesting to note that, while the vast majority of LINERs detected in the low-mass bin appears to take part in the evolutionary sequence, the presence of a second independent LINER population seems to emerge at intermediate masses. Fig. 10 reveals a clear dichotomy with a fair fraction of LINER-like objects that does not show signs of recent rejuvenation. This trend becomes even more evident at the highest masses, where the largest fraction of LINERs is detected (8 per cent), which contain only old stellar populations (see Fig. 9).

5.5 Dust properties along the sequence

Fig. 11 shows the stacked, normalised probability distribution functions for the dust parameter $E(B-V)$ obtained through our SED fitting algorithm for the low- and intermediate-mass bins. The different line-styles are the various emission line classes (see labels). As ought to be expected, dust content decreases along the sequence discussed above with highest dust attenuation in the star forming objects ($E(B-V) \sim 0.1$) and the lowest in the quiescent ones ($E(B-V) \lesssim 0.05$). This internal consistency further strengthens the conclusion that we are indeed observing a time sequence and are witnessing the transformation of early-type galaxies from star formation via AGN to quiescence. In order to mimic a time sequence in the observed $u-r$ colours with a variation in the amount

of dust rather than in age, the trend in $E(B-V)$ would have to be the opposite of what we observe.

6 DISCUSSION

With Figure 7 in Section 4 we show that early-type galaxies of different emission line classes occupy different loci in the colour-σ diagram. Star forming early-types are the bluest deviating most from the red sequence. Once some AGN contribution appears in the optical emission lines, the colours dramatically redden. In Section 5, we demonstrate quantitatively that there is indeed strong evidence for the existence of an evolutionary sequence of early-type galaxies moving from the blue cloud to the red sequence. We show that on this path the galaxies go through a number of phases starting at star formation followed by a transition region of star formation and AGN, a Seyfert AGN phase and a LINER phase before finally settling to total quiescence and passive evolution on the red sequence. This process is currently building the low-mass end of the red sequence in the low redshift universe. In this section we discuss the astrophysical implications of this finding, the role of LINER-like early-type galaxies, possible trigger mechanisms of this sequence, and follow-up observational campaigns in the context of the time sequence we have derived.

6.1 The starburst-AGN sequence

A clear implication of our results is the existence of a link between residual starburst and nuclear activity at recent epochs in low- and intermediate-mass early-type galaxies. Whatever triggers the starburst, it leads also to an AGN, and the star forming phase reaches quiescence via an AGN phase. We see the starburst fading while the AGN rises. This leads to two possible scenarios depending on whether the two processes, star formation and AGN, are connected.

6.1.1 AGN feedback or black hole growth in action?

If the fading of star formation and nuclear activity are linked, then we are observing AGN feedback in action. The appearance of the AGN in the transition region and Seyfert phases are concurrent with the end of star formation, so it is plausible that these two phenomena are connected such that the rise of the AGN suppresses and terminates star formation by heating and expulsion of the remaining gas.

Alternatively, it is possible that starburst and AGN actually do not interact with each other, even though they may be triggered by the same global event. In this case star formation fades simply owing to supernova feedback and/or the exhaustion of cold gas. Most interesting in the framework of this scenario is our finding that the AGN rises while star formation declines. This shows that in this case AGN activity must be delayed substantially with respect to the starburst by several hundred Myr and may actually be triggered by star formation. This implies that the early-type galaxy or its progenitor hosting the starburst is just in the process of building up its central super-massive black hole.

6.1.2 Gas depletion timescale: in favour of AGN feedback

In order to distinguish these two scenarios, we compare the observed timescale for the fading of star formation with simple theoretical estimates based on the Schmidt-Kennicutt law (Schmidt 1959; Kennicutt 1998). The latter relates the star formation rate with the ratio of gas mass surface density and the dynamical timescale of the system scaled by an efficiency ϵ. We assume that the dynamical timescale of star formation is on typical galaxy timescales of $\sim 0.1-0.5$ Gyr, as observed in gas discs in elliptical galaxies (Young 2002). We can exclude shorter dynamical timescales caused by a concentration of the star burst activity to small radii, as the mean petrosian half-light radii of the *u*-band light in the starforming early-types ($2.25''$) imply that star formation in these objects is extended over several kpc. Then to deplete any gas reservoir would take on the order of many Gyrs.

This timescale is significantly longer than the fading timescale deduced here for our sample galaxies. In our modelling analysis we find that the recent rejuvenation event is best modelled by a exponentially declining star burst with e-folding timescale around 100 Myr. Thus, the gas reservoir cannot get depleted *solely* via self-regulated star formation. An additional heating source is required. The fact that we find an AGN phase subsequent to the starburst strongly suggests that the AGN is (at least partly) responsible for the suppression of star formation by depleting the gas reservoir accelerating the transition from the blue cloud to the red sequence. A more detailed investigation of this process is beyond the scope of this paper. It will be explored in more detail in a forthcoming work (Kaviraj et al., in prep).

This argument strongly supports the AGN feedback interpretation of the time sequence. This result has important consequences for our understanding of galaxy formation. It is empirical proof that AGN feedback, the existence of which is now postulated in most recent models of hierarchical galaxy formation (see Introduction and references therein), occurs in early-type galaxies at late stages of their evolution. Beyond this important conclusion, our sample that is resolving the actual sequence of AGN feedback provides further insight into this process. We find its overall timescale to be of the order of a Gyr. Moreover, we observe a substantial delay between fading of star formation and rise of the AGN by a few hundred Myr, which might reflect the timescale required for the black hole to build up the accretion disc. This implies that AGN feedback is not well approximated with an immediate truncation as implicitly assumed in current hydrodynamical simulations (Springel et al. 2005a).

6.2 Obscured AGN?

A key result is that we see the AGN rising while star formation fades. As absolute O[III] luminosities increase along the sequence, it can be excluded that the AGN is simply out-shined by the starburst during the star forming phase. However, it is still possible that the AGN is not observed during the starburst, because it is highly obscured in the beginning. In this case, star formation and AGN would coexist from the beginning, and while star formation fades, the AGN remains active. This does not invalidate but rather strengthen the interpretation of AGN feedback occurring in our sample galaxies.

6.3 Progenitors and trigger mechanisms

The youngest early-type galaxies on the evolutionary sequence we resolve are the star forming ones with starburst ages around $100-200$ Myr. The progenitors of these objects within the sequence must have stellar populations younger than 200 Myr. The fact that we do not observe these objects implies that they are excluded through our selection criteria, hence they most likely do not have early-type morphology.

6.3.1 Prodigious star formation in the recent past

As we model the starburst as composite stellar population with exponentially declining star formation histories, these progenitors must have had significantly higher star formation rates in the past. The typical star forming early-type galaxy has a mass of about $5 \times 10^{10} M_{\odot}$ and has formed about 5% of its stellar mass in the current burst (i.e. $2.5 \times 10^{9} \mathrm{M}_{\odot}$) over the last 100 Myr. This corresponds to an *average* star formation rate of $25\ M_{\odot} yr^{-1}$, resulting in an infrared luminosity L_{IR} of $1.25 \times 10^{11} L_{\odot}$, well above the threshold for so-called luminous infrared galaxies (LIRGs). The star formation rate was undoubtedly higher in the past as the best fit decay timescale τ is around 100 Myr. Such an exponentially decaying star formation rate can easily boost the past L_{IR} into the category of ultra-luminous infrared galaxies (ULIRGs).

We find that the most luminous starforming early-type galaxy detected by the *Spitzer Space Telescope* in the *SDSS*-SWIRE overlap has $\mathrm{L_{FIR}} = 5.7 - 7.4 \times 10^{10}$ L$\odot$ (Sanders & Mirabel 1996) implying a star formation rate of $13\ M_{\odot} yr^{-1}$ based on the relationship of Gao & Solomon (2004). This galaxy is thus just slightly below the cut defining a LIRG of $L_{\mathrm{IR}} = 10^{11} L_{\odot}$ at the time it is observed.

We conclude that the progenitors of the objects we observe on the SF-AGN sequence were most likely ULIRGs. This fits well with the evidence that the local ULIRG population most likely will evolve into intermediate-mass early-type galaxies (Genzel et al. 2001). Dasyra et al. (2006a, 2006b) and Veilleux et al. (2006) have analysed HST H-band imaging and VLT spectra of low redshift ULRIGs and QSOs and concluded that while most of them are ongoing mergers, their kinematic, structural, and photometric properties are consistent with them becoming elliptical galaxies and settling on the fundamental plane. Most relevant here is that they find their stellar velocity dispersions to have typical values of around $150\ \mathrm{kms}^{-1}$ in overlap with the typical velocity dispersions of our active galaxies that mark the transformation process from blue cloud to red sequence.

The appearance of an AGN phase several hundred Myr *after* the U/LIRG phase may explain why most local ULIRGs do not appear to contain a luminous AGN (Genzel et al. 1998).

6.3.2 Merger as main trigger

The origin of ULIRG activity is thought to be a galaxy merger (e.g. Genzel et al. 2001). This implies that we are possibly seeing a slightly more advanced stage of a gas-rich merger where the morphology has already settled into a spheroid, and the infrared luminosity has already decayed below the LIRG threshold.

Because of our sample selection, all objects discussed here are morphologically early-type galaxies without spiral or disc structure as far as detectable in the *SDSS* images. Elliptically shaped galaxies with minor morphological perturbations such as tidal features or dust lanes are *not* excluded. This selection should in principle enable us to investigate the role of morphological disturbance, hence merger and galaxy interaction activity, along the sequence. However, the fraction of disturbed early-type galaxies in our sample is quite small. We have not found any compelling trend between morphological irregularities and star formation/nuclear activity, most likely because SDSS imaging does not provide the necessary sensitivity in terms of depth and spatial resolution. Deeper imaging, preferably at higher spatial resolution, is clearly needed to identify signatures of recent merger activity in our sample objects (see e.g., van Dokkum 2005 and Bell et al. 2006).

6.4 Eddington ratios along the sequence

In the following we discuss the nature of accretion onto the supermassive black hole along the AGN feedback sequence. In Figure 12, we show the distributions of [OIII] luminosity and the quantity L[OIII]/σ^4 for Seyfert, low-mass and high-mass LINERs. L[OIII]/σ^4 has been introduced by Kewley et al. (2006) as a tracer of the Eddington ratio assuming that [OIII] luminosity scales with the AGN bolometric luminosity (Heckman et al. 2004), and that σ^4 provides an estimate of the central super-massive black hole mass (Gebhardt et al. 2000; Ferrarese & Merritt 2000). Based on this quantity Kewley et al. (2006) show that the fundamental difference between Seyferts and LINERs in the *SDSS* data base is the accretion efficiency, with the LINERs being at lower Eddington ratios than the Seyferts. Since the transition region objects [OIII] line luminosities have some contribution from star formation, we can treat them as upper limits on both the accretion rate and efficiency.

We find that the Seyfert early-types in our sample are high-luminosity AGN with high L[OIII] luminosities and high L[OIII]/σ^4 ratios, indicating that they are strongly accreting systems relatively close to the Eddington limit. The LINERs, instead, have lower L[OIII] luminosities and lower Eddington ratios. There is an interesting trend with mass, however. The massive LINERs exhibit the lowest accretion rates, while the low- and intermediate-mass objects are found between massive LINERs and Seyferts. Hence our low-mass and high-mass LINER early-type galaxies are objects in different states of nuclear activity. The former represent probably the end stage of the SF-AGN sequence. If the Seyfert phase is a high-accretion phase during which the AGN feedback process occurs, then the transition to the LINER phase is the point at which the supply of gas has been largely used up by star formation and/or accretion onto the black hole. The massive LINERs characterised by low Eddington ratios, instead, might be responsible (or at least part of) the rigourous AGN feedback process in massive early-type galaxies that avoid rejuvenation in the first place. Figure 12 illustrates the extended rise and decline in both accretion rate and Eddington ratio over the time domain covered by the time sequence. While the transition region to Seyfert evolution brings with it an increase in accretion, so the progression to a LINER is accompanied by a decline.

6.5 The role of LINERs

Fig. 9 shows that the fraction of LINERs observed increases with increasing galaxy mass, while the fraction of galaxies undergoing the SF-AGN sequence decreases. Hence, LINERs appear to come in two flavours. Some are part of the evolutionary sequence of low- and intermediate-mass galaxies, but the majority is found in the massive, quiescent early-type galaxies of our sample.

It should be emphasised that the LINER-like emission observed here is most likely caused by nuclear activity. The extended LINER-like emission not associated with an AGN found by Sarzi et al. (2006) in very nearby early-type galaxies is significantly weaker (typically with total L[OIII] $< 10^{6} \mathrm{L}_{\odot}$; c.f. Figure 12) and would remain undetected in our sample.

6.5.1 LINERs in low and intermediate masses

As discussed in the previous sections, the early-type galaxies with LINER emission appear on the evolutionary sequence of low- and intermediate-mass objects between Seyfert-like nuclear activity and quiescence. This means that early-type galaxies transition from

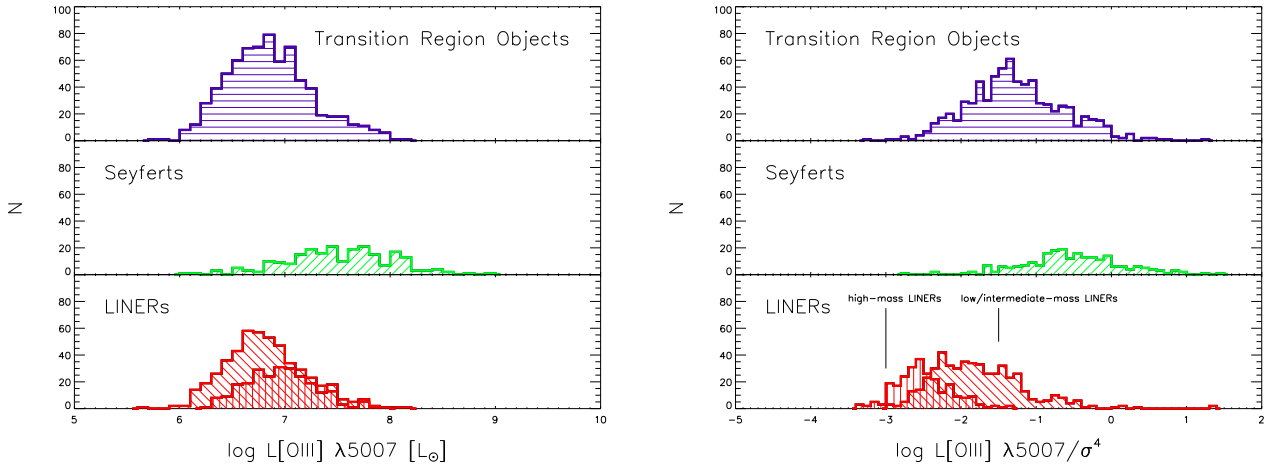

Figure 12. In the left-hand part of this Figure, we show the histograms for the L[OIII] λ5007 luminosities of our AGN and transition region objects. [OIII] is a tracer of the accretion rate (Heckman et al. 2004) and so is an upper limit on the accretion rate of the transition region objects. In the left-hand part, we show the histogram of the quantity L[OIII]/σ^4, which is proportional to the Eddington ratio (Kewley et al. 2006). In each part, we go along the sequence from early times to late. First, we show the transition region objects, then the Seyferts and then the LINERs. We split the LINERs into two; while the low- and intermediate-mass LINERs and the high-mass LINERs have similar [OIII] luminosities, their Eddington ratios are very different. The low/intermediate-mass LINERs form the low luminosity and high Eddington ratio end of the Seyfert distribution, as would be expected from their place in the time sequence. The high-mass LINERs have Eddington ratios an order of magnitude below their lower-mass counterparts. Along the sequence, both absolute L[OIII] and Eddington ratio rise, peak and then decline over the time domain covered by the time sequence.

a high-accretion regime characterised by Seyfert-emission to a low accretion regime characterised by LINER-emission (Kewley et al. 2006) as they proceed to fade onto the red sequence. This can be interpreted as the AGN running out of fuel. This is well consistent with the study of Yan et al. (2006), who find that many post-starburst galaxies show strong [OII] emission, but no Hα, indicating no further ongoing star formation, which they associate with LINERs.

6.5.2 *LINERs in massive galaxies*

Already in the intermediate mass bin, most LINERs appear to be associated with stellar quiescence (Figure 9), and none of the LINERs in the highest mass bin are connected with rejuvenation. This might be AGN feedback in its most rigourous form and is consistent with the fact that the efficiency of AGN feedback must increase with increasing galaxy mass in the models in order to reproduce observed UV colours (Schawinski et al. 2006b). While late star formation seems to be terminated by nuclear activity in low-mass early-type galaxies, the AGN in massive galaxies may prevent star formation in the first place. These massive galaxies most likely have experienced strong AGN feedback at high accretion nuclear activity at earlier epochs. Indeed, observational evidence for the existence of this process has recently been found (Kriek et al. 2006; Rodighiero et al. 2007b; Daddi et al. 2007).

This LINER-like activity may play the crucial role in maintaining an atmosphere of hot X-ray emitting gas which can shield the galaxy from gas accretion and cooling and so prevent any further star formation as suggested by Binney (2004). Such hot gas may then trigger *extended* LINER-like emission via thermal conduction of self-irradiation as has been seen in massive nearby elliptical galaxies (see e.g Sarzi et al. 2007 and references therein), although it is likely that the majority of the LINER emission in our sample is associated with (more luminous) nuclear activity.

6.5.3 *Mis-classified LINERs*

We note that some transition region early-types are found in the highest mass bin, which show no evidence for a star formation episode (see Fig. 9). These transition region objects, being the result of a combination of star formation and AGN activity, have no corresponding starforming or Seyferts at the same mass and do not seem to take part in the AGN-SF time sequence. Instead, their properties are far more similar to those of high-mass LINERs. The most likely explanation for this apparent contradiction is that the extreme starburst line of Kewley et al. (2001) led to the mis-classification of some LINERs as transition region objects. An improved classification scheme including the low-ionisation lines may help here but is beyond the scope of this paper.

6.6 Follow-up observations

The sample presented in this paper is the ideal laboratory for more detailed follow-up studies of the link between star formation and nuclear activity in early-type galaxies. Multi-wavelength data will tighten constraints on the formation histories, the star formation activities, dust contents, central black hole activities, and accretion rates of our sample galaxies. This will provide deeper insight into the physics involved.

By observing CO molecular transitions the fate of the molecular gas can be explored. Such observations clarify whether it is really is the feedback from AGN that quenches star formation, or whether this decline in star formation is caused by the fuel supply being exhausted by star formation itself. High-resolution radio continuum observations at different frequencies provide important clues on the relative contributions of star formation and the AGN along the sequence. The relative importance and interaction between AGN and star-formation in the galaxies along our timeline can be further addressed by the analysis of the full SED in the mid-infrared wavelength regime. Mid-infrared imaging helps to pin down the relative amounts of cold, warm and hot dust, while spec-

troscopy can disentangle contributions from PAH lines to any hotter dust components due to an AGN. Finally, deep optical imaging would be very valuable and help to determine the role of mergers and interactions along the AGN feedback sequence.

Observations at the observatory of the Institut de Radioastronomie Milimetrique (IRAM) and at the Very Large Array (VLA) to address part of these questions have been taken in June and July 2007.

7 CONCLUSIONS

We study the relationship between star formation and nuclear activity in early-type galaxies at recent epochs. The principle aim is to test whether AGN feedback occurs in these objects, as invoked in most recent models of hierarchical galaxy formation.

For this purpose, we analyse a magnitude-limited sample of 48,023 galaxies drawn from the *SDSS* DR4 in the redshift range of 0.05 to 0.1 limited to $r < 16.8$. We visually inspected all galaxies in this sample identifying 15,729 morphological early-type galaxies. This paper is the first of a project called MOSES: **MO**rphologically **S**elected **E**llipticals in **S**DSS. A detailed description of the catalogue can be found in a companion paper (Schawinski et al., in preparation). Most importantly, the MOSES sample is not biased against star formation and nuclear activity thanks to the purely morphological selection criterion. The SDSS photometry is matched to a number of other surveys, namely *GALEX*, *2MASS*, and *SWIRE*, yielding a wavelength coverage from the far-UV to mid-IR. Reanalysing the *SDSS* spectra, we measure emission line fluxes, stellar absorption line indices and velocity dispersions. The contributions of the stellar continuum and of the ionised-gas emission to the observed galaxy spectrum are separated by fitting *simultaneously* stellar population templates.

18.4 per cent of the early-type galaxies in our sample show emission lines, and we employ emission line ratio (BPT) diagrams to classify them into starforming, AGN-SF composites, Seyfert AGN and LINERs. The fraction of emission line galaxies increases with decreasing galaxy mass to 40 per cent at the low-mass end ($\sigma < 100\ \mathrm{kms}^{-1}$). The emission line classes are roughly evenly distributed between star formation and AGN at intermediate ($100 < \sigma \leqslant 200$ km/s) and low ($\sigma \leqslant 100$ km/s) masses. At high masses ($\sigma > 200$ km/s), instead, only LINER-like emission is detected. The Hα star formation rates of those objects classified as currently star forming range from $0.1 - 25\ \mathrm{M}_{\odot}\mathrm{yr}^{-1}$.

We find that the objects with emission are offset from the red sequence and form a well-defined pattern in the colour-σ diagram. Star forming early-types inhabit the blue cloud, while early-types with AGN (Seyfert and LINER) are located considerably closer to and almost on the red sequence. Star formation-AGN composites are found right between these two extremes. There is a sequence between the blue cloud and the red sequence from star forming via transition region and Seyfert AGN and LINER to quiescence.

To analyse this transition in more detail, we have developed a method for deriving star formation histories with particular focus on quantifying the epoch and mass fraction of the last significant episode of star formation. Novel about our approach is to use a combination of UV-optical-NIR photometry and stellar absorption indices as observational constraints.

We find that low- and intermediate-mass early-type galaxies with emission lines have experienced an episode of star formation less than ~ 1 Gyr ago involving $1-10$ per cent of their total stellar mass. This recent star burst is best modelled by a steeply declining exponential with e-folding timescale around 100 Myr. Most importantly, this timescale and the mass fraction involved is the same for all the emission line early-type galaxies whether they are star-forming, Transition Region, Seyferts or LINERs. They are offset in time, however, with the starforming being the youngest, and the Seyfert/LINERs being the oldest. Quiescent galaxies (objects without emission lines) have star burst ages larger than 1 Gyr, which sets the timescale for the transition process we observe. The duration of the various phases along this sequence agree reasonably well with the number fractions observed, once geometric effects of Seyfert activity are taken into account. Dust content decreases along the sequence with highest dust attenuation in the star forming objects ($E(B-V) \sim 0.1$) and the lowest in the quiescent ones ($E(B-V) \lesssim 0.05$).

These results lead to the conclusion that we are observing an evolutionary sequence and are witnessing the transformation of early-type galaxies from star formation via AGN to quiescence. Along this sequence, nuclear activity rises while star formation fades. We discuss that gas exhaustion or self-regulation of star formation alone does not suffice to explain this fading, which leads to the conclusion that we have detected a sequence in which nuclear activity suppresses star formation. We are seeing AGN feedback in action, while low- and intermediate-mass early-type galaxies transition from the blue cloud through the green valley, characterised by nuclear activity, onto the red sequence. The high-mass galaxies in our sample, instead, did not go through this transition in the recent past. These objects have only LINER-like emission and are not associated with rejuvenation. This indicates that the AGN in massive galaxies may prevent star formation in the first place, which would be AGN feedback in its most rigourous form.

To conclude, we have found empirical evidence for the occurrence of AGN feedback in early-type galaxies at recent epochs. The galaxy sample presented here is the ideal laboratory for testing more detailed physics of this process. A first important hint from this work is that there is a substantial delay between fading of star formation and rise of the AGN by a few hundred Myr. This implies that AGN feedback is not well approximated with an immediate truncation as implicitly assumed in current models.

ACKNOWLEDGEMENTS

We would like to thank the referee for the thorough and prompt report. We thank Andi Burkert, Stephen Justham, Sadegh Khochfar, Chris Lintott, Lance Miller, Dimitra Rigopouplou, Clive Tadhunter and Roberto Trotta for many stimulating discussions. We would also like to thank Stephen Justham and Philipp Podsiadlowski for letting us use their computing resources.

This project has been partly supported by grant BMBF-LPD 9901/8-111 of the Deutsche Akademie der Naturforscher Leopoldina. SK acknowledges a Leverhulme Early-Career Fellowship, a BIPAC fellowship and a Research Fellowship from Worcester College, Oxford. SJJ was supported by the Korea Research Foundation Grant funded by the Korean Government (MOEHRD) (KRF- 2005-213-C00017). CM ackwnoledges the grant MEIF-CT-2005-011566 of the Training and Mobility of Researchers programme financed by the European Community.

The SDSS is managed by the Astrophysical Research Consortium (ARC) for the Participating Institutions. The Participating Institutions are the University of Chicago, Fermilab, the Institute for Advanced Study, the Japan Participation Group, The Johns Hopkins University, the Korean Scientist Group, Los Alamos National

Laboratory, the Max-Planck-Institute for Astronomy (MPIA), the Max-Planck-Institute for Astrophysics (MPA), New Mexico State University, University of Pittsburgh, University of Portsmouth, Princeton University, the United States Naval Observatory, and the University of Washington.

This publication makes use of data products from the Two Micron All Sky Survey, which is a joint project of the University of Massachusetts and the Infrared Processing and Analysis Center/California Institute of Technology, funded by the National Aeronautics and Space Administration and the National Science Foundation.

REFERENCES

Adelman-McCarthy J. K. et al. 2006, ApJS, 162, 38
Allen C. W., 1976, Astrophysical Quantities. Astrophysical Quantities, London: Athlone (3rd edition), 1976
Baldwin J. A., Phillips M. M. & Terlevich R., 1981, PASP, 93, 5
Bell E. F. et al. 2006, ApJ, 640, 241
Bennett C. L. et al. 2003, ApJS, 148, 1
Benson A. J. et al. 2003, ApJ, 599, 38
Bernardi M. et al. 2006, AJ, 131, 1288
Bernardi M. et al. 2003a, AJ, 125, 1817
—, 2003b, AJ, 125, 1849
—, 2003c, AJ, 125, 1866
Bernardi M. et al. 2003d, AJ, 125, 1882
Best P. N., Kaiser C. R., Heckman T. M., Kauffmann G., 2006, MNRAS, 368, L67
Best P. N. et al. 2005, MNRAS, 362, 25
Binney J., 2004, MNRAS, 347, 1093
Birnboim Y., Dekel A., Neistein E., 2007, ArXiv Astrophysics e-prints
Blanton M. R. et al. 2003a, AJ, 125, 2348
Blanton M. R. et al. 2003b, AJ, 125, 2276
Blanton M. R. et al. 2005, AJ, 129, 2562
Bouchet P. et al. 1985, A&A, 149, 330
Bower R. G. et al. 2006, MNRAS, 370, 645
Caldwell N., Rose J. A. & Concannon K. D., 2003, AJ, 125, 2891
Calzetti D. et al. 2000, ApJ, 533, 682
Cappellari M., Emsellem E., 2004, PASP, 116, 138
Carson D., 2007, Phd thesis, University of Portsmouth, Portsmouth
Cattaneo A. et al. 2007, MNRAS, 377, 63
Cattaneo A. et al. 2006, MNRAS, 370, 1651
Cavaliere A., Menci N., 2007, ArXiv e-prints, 704
Cimatti A., Daddi E. & Renzini A., 2006, A&A, 453, L29
Ciotti L. & Ostriker J. P., 1997, ApJ, 487, L105+
Combes F., Young L. M. & Bureau M., 2007, ArXiv Astrophysics e-prints
Connolly A. J. & Szalay A. S., 1999, AJ, 117, 2052
Croton D. J. et al. 2006, MNRAS, 365, 11
Daddi E. et al. 2007, ArXiv e-prints, 705
Dasyra K. M. et al. 2006a, ApJ, 638, 745
Dasyra K. M. et al. 2006b, ApJ, 651, 835
De Lucia G. et al. 2006, MNRAS, 366, 499
Dekel A. & Silk J., 1986, ApJ, 303, 39
Di Matteo T. et al. 2007, ArXiv e-prints, 705
Di Matteo T., Springel V. & Hernquist L., 2005, Nature, 433, 604
Eisenstein D. J. et al. 2001, AJ, 122, 2267
Faber S. M. et al. 2005, ArXiv Astrophysics e-prints
Fabian A. C. et al. 2005, MNRAS, 360, L20
Fabian A. C. et al. 2006, MNRAS, 366, 417
Ferrarese L. & Merritt D., 2000, ApJ, 539, L9
Ferreras I. & Silk J., 2000, ApJ, 541, L37
Fitzpatrick E. L., 1986, AJ, 92, 1068
Fukugita M. et al. 1996, AJ, 111, 1748
Fukugita M. et al. 2007, AJ, 134, 579
Fukugita M. et al. 2004, ApJ, 601, L127
Gao Y. & Solomon P. M., 2004, ApJ, 606, 271
Gebhardt K. et al. 2000, ApJ, 539, L13
Genzel R. et al. 1998, ApJ, 498, 579
Genzel R. et al. 2001, ApJ, 563, 527
Granato G. L. et al. 2004, ApJ, 600, 580
Granato G. L. et al. 2001, MNRAS, 324, 757
Graves G. J. et al. 2007, ArXiv e-prints, 707
Gunn J. E. et al. 1998, AJ, 116, 3040
Harris G. L. H. & Harris W. E., 2000, AJ, 120, 2423
Harris G. L. H., Harris W. E. & Poole G. B., 1999, AJ, 117, 855
Harris W. E., Harris G. L. H., 2002, AJ, 123, 3108
Heckman T. M. et al. 2004, ApJ, 613, 109
Hopkins P. F. et al. 2007, ArXiv e-prints, 706
Jimenez R. et al. 2006, ArXiv Astrophysics e-prints
Kauffmann G. & Charlot S., 1998, MNRAS, 294, 705
Kauffmann G. et al. 1999, MNRAS, 303, 188
Kauffmann G. et al. 2006, ArXiv Astrophysics e-prints
Kauffmann G. et al. 2003, MNRAS, 346, 1055
Kaviraj S. et al. 2005, MNRAS, 360, 60
Kaviraj S. et al. 2006, Accepted for 2nd GALEX ApJS Issue
Kawata D. & Gibson B. K., 2005, MNRAS, 358, L16
Kennicutt Jr. R. C., 1998, ApJ, 498, 541
Kewley L. J. et al. 2001, ApJ, 556, 121
Kewley L. J. et al. 2006, MNRAS, 372, 961
Khochfar S. & Ostriker J. P., 2007, ArXiv e-prints, 704
Kriek M. et al. 2006, ArXiv Astrophysics e-prints
Lonsdale C. J. et al. 2003, PASP, 115, 897
MacArthur L. A., 2005, ApJ, 623, 795
Maraston C., 1998, MNRAS, 300, 872
—, 2005, MNRAS, 362, 799
Maraston C. & Thomas D., 2000, ApJ, 541, 126
Martin D. C. et al. 2005, ApJ, 619, L1
Martin D. C. et al. 2007, ArXiv Astrophysics e-prints
Morganti R. et al. 2006, MNRAS, 371, 157
Nagashima M. et al. 2005, MNRAS, 363, L31
Nandra K. et al. 2007, ApJ, 660, L11
Nelan J. E. et al. 2005, ApJ, 632, 137
Panter B., Heavens A. F. & Jimenez R., 2003, MNRAS, 343, 1145
Panter B. et al. 2006, ArXiv Astrophysics e-prints
Prevot M. L. et al. 1984, A&A, 132, 389
Rodighiero G. et al. 2007a, ArXiv Astrophysics e-prints
Rodighiero G. et al. 2007b, MNRAS, 376, 416
Salim S. et al. 2007, ArXiv e-prints, 704
Sanders D. B. & Mirabel I. F., 1996, ARA&A, 34, 749
Sarajedini A. & Jablonka P., 2005, AJ, 130, 1627
Sarzi M. et al. 2007, New Astronomy Review, 51, 18
Sarzi M. et al. 2006, MNRAS, 366, 1151
Schawinski K. et al. 2006a, Accepted for 2nd GALEX ApJS Issue
Schawinski K. et al. 2006b, Nature, 442, 888
Schmidt M., 1959, ApJ, 129, 243
Sijacki D. et al. 2007, ArXiv e-prints, 705
Silk J., 2005, MNRAS, 364, 1337
Silk J. & Rees M. J., 1998, A&A, 331, L1
Skrutskie M. F. et al. 2006, AJ, 131, 1163

Springel V., Di Matteo T. & Hernquist L., 2005a, MNRAS, 361, 776
Springel V. et al. 2005b, Nature, 435, 629
Springel V. et al. 2001, MNRAS, 328, 726
Stasińska G. et al. 2006, MNRAS, 371, 972
Stoughton C. et al. 2002, AJ, 123, 485
Sutherland R. S. & Dopita M. A., 1993, ApJS, 88, 253
Thomas D., 1999, MNRAS, 306, 655
Thomas D., Maraston C. & Bender R., 2003, MNRAS, 339, 897
Thomas D. et al., 2005, ApJ, 621, 673
Thomas D., Maraston C. & Korn A., 2004, MNRAS, 351, L19
Trager S. C. et al. 2000, AJ, 120, 165
Trager S. C. et al. 1998, ApJS, 116, 1
Tremonti C. A. et al. 2004, ApJ, 613, 898
van Dokkum P. G., 2005, AJ, 130, 2647
Veilleux S. et al. 2006, ApJ, 643, 707
Wake D. A. et al. 2006, MNRAS, 372, 537
White S. D. M. & Frenk C. S., 1991, ApJ, 379, 52
Wild V. et al. 2007, ArXiv e-prints, 706
Worthey G. et al. 1994, ApJS, 94, 687
Worthey G. & Ottaviani D. L., 1997, ApJS, 111, 377
Yan R. et al. 2006, ApJ, 648, 281
Yi S. K. et al. 2005, ApJL, 619, L111
York D. G. et al. 2000, AJ, 120, 1579
Young L. M., 2002, AJ, 124, 788

This paper has been typeset from a TEX/ LATEX file prepared by the author.